Date: August 7, 1995

To: Harry Montgomery / NASA
I.L. Goldberg / Swales

From: Daniel S. Knowles Jr./GSC

Subject: MODIS Infrared Calibration Algorithm Derivation for ATBD 1995: Draft Copy

Infrared detection must be addressed from the point of view of the detector since a majority of the detector incident radiant flux originates from within the optical system.

1. Calibration Coefficients

This algorithm expands on the ideas of both I.L. Goldberg and T. Pagano. Through careful mathematical manipulation of the terms of the fundamental detector incident radiant flux equation presented in this document, all neccessary parameters can be sufficiently determined on-orbit with just two calibrators. These parameters are determined as a group and not individually and the groups are refered to as "calibration coefficients".

A MODIS infrared calibration coefficient is a deliberate mathematical grouping of the individual parameters of the pre-amplified focal plane voltage relationship to the detector incident radiant flux, considered invariant for a period of one scan line, not directly measured, but determined from the telemetry pertaining to a relevant reference radiance source. These coefficients will be continuously adjusted on-orbit to correct for change since the pre-launch measurements.

2. MODIS Overview

MODIS uses HgCdTe detectors, operating at a temperature of 85 Kelvin, to sense radiation in the infrared portion of the radiometric spectrum. Each IR wavelength band has ten detectors in parallel (along track). The signal path from an individual detector to the output is called a channel. Each detector has a 1 kilometer Instantaneous Field Of View (IFOV) when imaging the Earth at nadir. Each band has a filter, also at 85 Kelvin, to permit a limited spectral range to irradiate its 10 constituant detectors. There are 16 infrared bands on the MODIS instrument with center wavelengths ranging from 3.75 μm to 14.235 μm (see Table 1). The short to midwave infrared bands (MODIS bands 20-25, 27-30) use photovoltaic detectors. The long wave infrared bands (MODIS bands 31-36) use photoconductive detectors.

MODIS uses two on-orbit calibrators (a blackbody and a view of space) as reference targets from which it determines the spectral radiance emitted from the Earth and its atmosphere. A paddle wheel scan mirror is used to scan the optical line of sight of the detectors across the calibrators and the Earth's surface. The scan mirror is two sided, each side completing a scan with 180 degrees of mirror rotation. The duration of one scan (180 degree rotation of the scan mirror) is 1.4 seconds.

MODIS will be affixed to the EOS AM and EOS PM spacecraft (see Fig. 0). The AM series will have a descending sun-synchronous orbit with an equatorial crossing time of 10:30 AM. The PM series will have a ascending sun-synchronous orbit with an equatorial crossing time of 1:30 PM. The orbital altitude will be 705.3 km with a 98.21 degree inclination.

Band	Center Wavelength
20	3.750μm
21	3.959μm
22	3.959μm
23	4.050μm
24	4.465μm
25	4.515μm
27	6.715μm
28	7.325μm
29	8.550μm
30	9.730μm
31	11.030μm
32	12.020μm
33	13.335μm
34	13.635μm
35	13.935μm
36	14.235μm

Table 1. MODIS center wavelengths

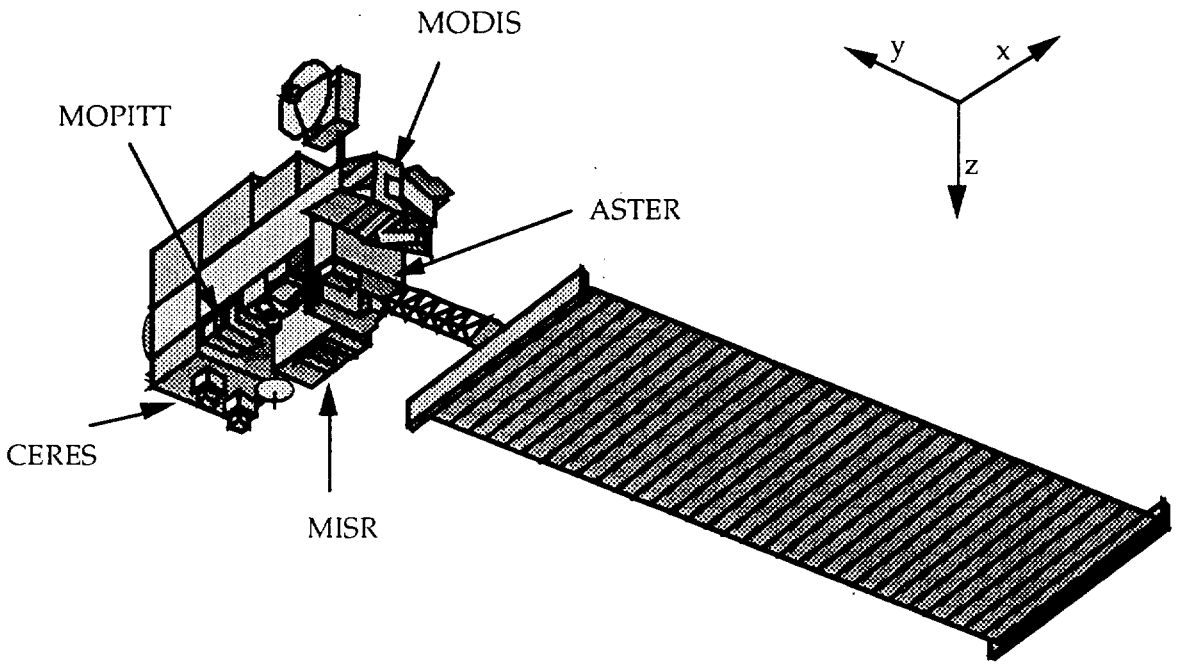

Figure 0. EOS AM & EOS PM Spacecraft

The velocity vector of the EOS AM spacecraft is defined as the positive x direction. The axis of the MODIS scan mirror is aligned with the x axis. The rotation of the scan mirror is in the positive x direction as defined by the right hand rule. The view point of Figures 1 - 3, which is a cutout view of the key infrared components in the MODIS scan cavity, is such that the scan mirror rotates in the clockwise direction. The vector extending from the scan mirror axis to approximately the center of the Earth view porthole defines the positive z direction. During normal spacecraft operations, the positive z direction will be aligned with Earth nadir.

As the scan mirror rotates in the positive x direction, an angle is traced out between the optical line of sight and the positive z axis. This angle is referred to as the MODIS scan (or view) angle. This angle extends across 360 degrees of geometric space for 180 degrees of mirror rotation. The optical axis is located at an angle of 284 degrees with respect to the positive z axis.

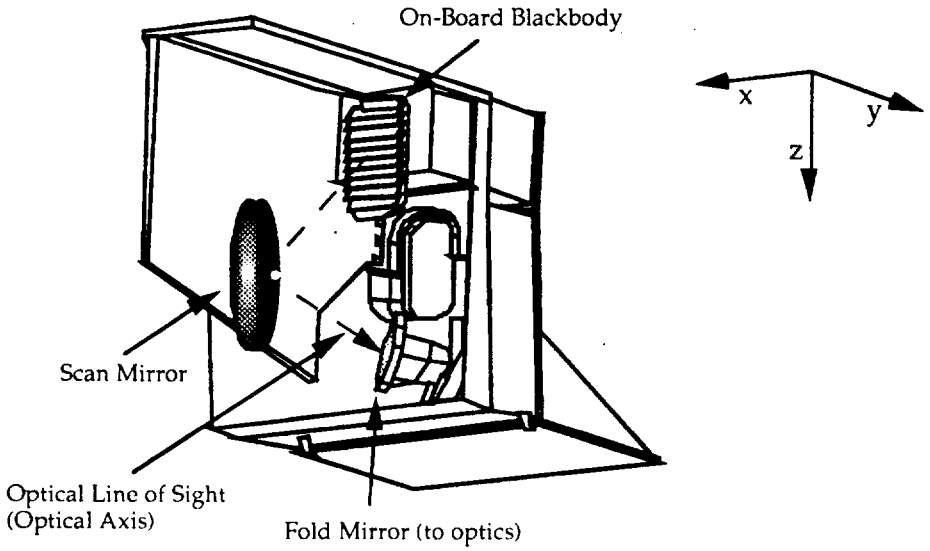

Figure 1. MODIS scan of the on-board blackbody

The first calibrator of concern to infrared calibration is the on-board blackbody. This is a v-groove structure constructed of anodized aluminum with 12 embedded thermistors. According to the MODIS specification for the on-board blackbody, the emissivity will be no less than .992, known to .004 with an effective blackbody temperature known to .1 Kelvin. The on-board blackbody is the "hot" calibration target with an ambient operating temperature of 285 Kelvin, and an optional heated mode temperature of 315 Kelvin. The scan mirror has a nominal view angle 231.4 degrees while imaging the blackbody with a nominal angle of incidence between the optical axis and the scan mirror normal of 50.25 degrees. MODIS collects 15 data points during each scan of the blackbody covering an angular span of 16 IFOV. Figure 1 illustrates the scan mirror positioning and optical line of sight while MODIS is imaging the on-board blackbody.

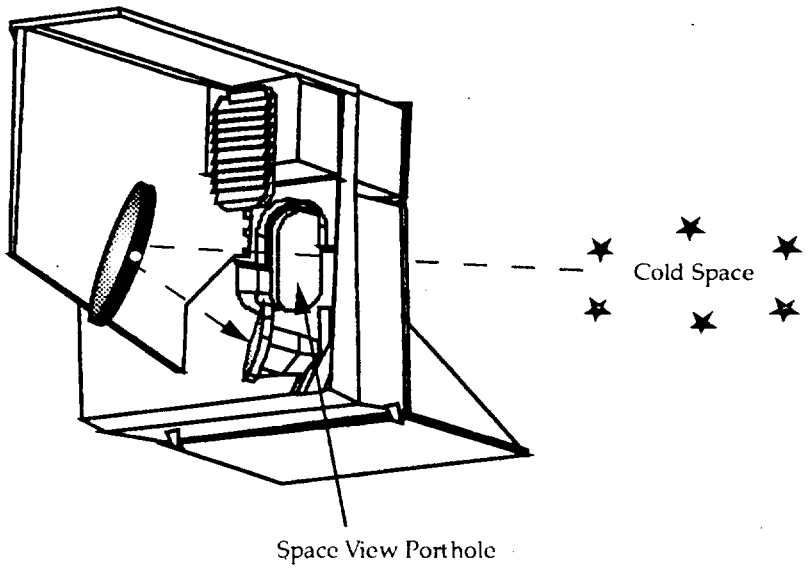

Figure 2. MODIS scan of the space view

The second calibrator of concern to infrared calibration is the space view. This is a porthole in the MODIS cavity which has a direct view of space. Space is the "cold" calibration target with an effective temperature on the order of 3 Kelvin. The scan mirror has a nominal view angle of 261.2 degrees while imaging the space view with a nominal angle of incidence between the optical axis and the scan mirror normal of 11.42 degrees. MODIS collects 15 data points during each scan of the space view covering an angular

span of 16 IFOV. Figure 2 illustrates the scan mirror positioning and optical line of sight while MODIS is imaging space through the space view porthole.

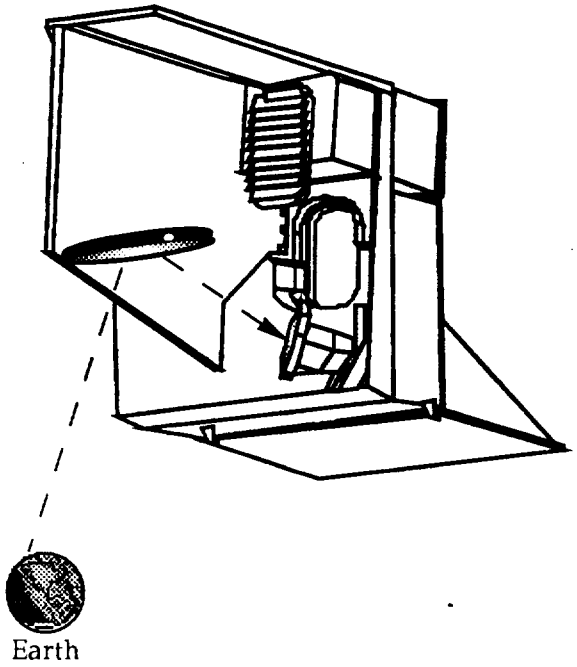

Figure 3. MODIS scan of the Earth

The third important infrared region in the MODIS scan is the scan of the Earth through the Earth view porthole. The scan mirror begins the scan of Earth with a nominal view angle of -55 degrees and a nominal angle of incidence between the optical axis and the scan mirror normal of 10.5 degrees. The scan mirror ends the scan of Earth with a nominal view angle of 55 degrees and a nominal angle of incidence between the optical axis and the scan mirror normal of 65.5 degrees. 1354 data points are collected corresponding to an angular span of 1355 IFOV. Figure 3 illustrates the scan mirror positioning and optical line of sight while MODIS is imaging an Earth scene through the Earth view porthole.

The scan mirror has a reflectivity which significantly varies with scan angle. This is primarily due to the SiOx coating on the mirror. Due to this phenomena, a rather complex calibration algorithm is needed to correct for this angular reflectivity variation of the scan mirror. This neccesitates a full roll of the spacecraft during orbit in order to view space through the entire Earth view porthole. The signal variations during this view of a "uniform" target will provide the means to correct for errors in the pre-launch measurement of the scan mirror reflectivity as well as correct for the effects of contamination across the mirror's surface. The contamination for larger Earth view angles is expected to be greater than for the smaller angles. This is because the larger angle has a focal plane "footprint" which extends closer to the edges of the scan mirror, which span more space than the center regions.

3. The Master Curve Approach

The MODIS infrared calibration algorithm uses a quadratic fit on the detector incident radiant flux to pre-amplified voltage transfer curve in order to determine the mean spectral radiance of an Earth scene source. This fit may not be quadratic over the entire range of possible detector incident radiant flux, but, it should provide a good fit over the somewhat limited flux range which we plan to use. The region of the curve which passes through P_{back} (see Fig. 4) is actually an extrapolation of the quadratic fit from the useable radiant flux range of the space view (sv), Earth view (ev), and the on-board blackbody (bb) image sources. This will be verified in the thermal vacuum testing. This approach is referred to as the master curve approach. The shape of this curve may vary from scan to scan due to gain changes of the detector. To correct for this, the "gain" of the curve and offset due to the optical background flux will be determined every scan, whereas the "non-linearity" of the curve will be treated as a constant. This assumption is required due to the shortage of on-orbit calibrators. The non-linearity of HgCdTe is typically on the order of about 1%

and will be determined pre-launch for each detector. For MODIS, SBRC has claimed that the nonlinearity could be as high as 5% for the PV and 10% for the PC bands.

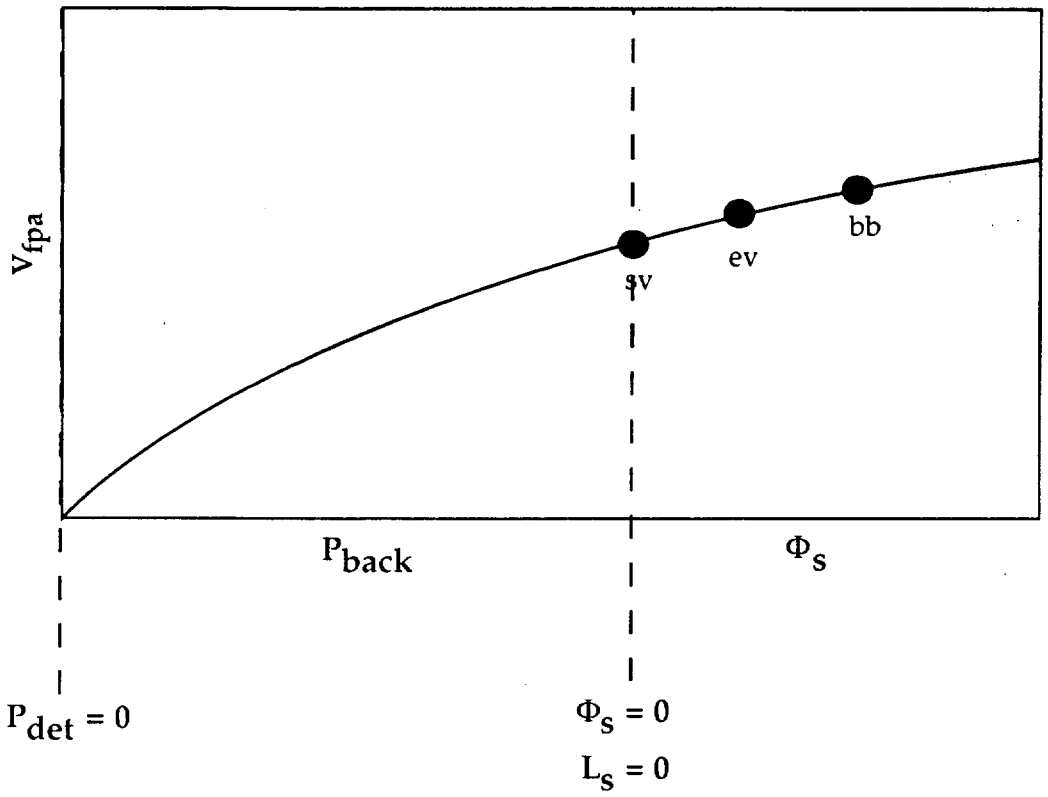

Figure 4. MODIS Infrared Master Calibration Curve

The pre-amplified voltage may therefore be expressed in terms of the detector power as

$$V_s = a(\Phi_s + P_{back})^2 + b(\Phi_s + P_{back}) \quad (1)$$

where

Φ_s detector incident radiant flux (power) attributed solely to the scan mirror and scene

P_{back} extrapolated detector background power attributed to the temperature of the optics and the bias voltage

Since MODIS applies differing gains and offset voltages every scan, the master curve approach cannot be in terms of MODIS counts. MODIS counts have no meaning without their respective applied gains and offset voltage values. Therefore, the master curve will be expressed in terms of the pre-amplified voltage across the load resistor for the photoconductive bands and the pre-amplified voltage across the detector for the photovoltaic bands. This differentiation is useful since we desire these pre-amplified voltages to increase with an increase in detector flux for both the PC and PV bands, thereby enabling the equation to apply equally to both bands.

For a full aperture optical system of transmission $\tau_{\lambda,opt}$, the detector incident radiant flux due solely to an external Lambertian source $L_{\lambda,lamb}$ can be expressed as

$$\Phi_s = \frac{\pi A_d}{4\left(f^{\#}_{eff}\right)^2_{port}} \int_{\lambda=0}^{\infty} L_{\lambda,lamb}\tau_{\lambda,opt}d\lambda \tag{2}$$

where A_d is the image area of the detector and $f^{\#}_{eff}$ is the effective focal ratio, which for a symmetrical optical system and an unimmersed detector is defined as:

$$f^{\#}_{eff} = \frac{1}{2\sin\phi_{port}} \tag{3}$$

where ϕ_{port} is the acceptance angle (see Fig. 5).

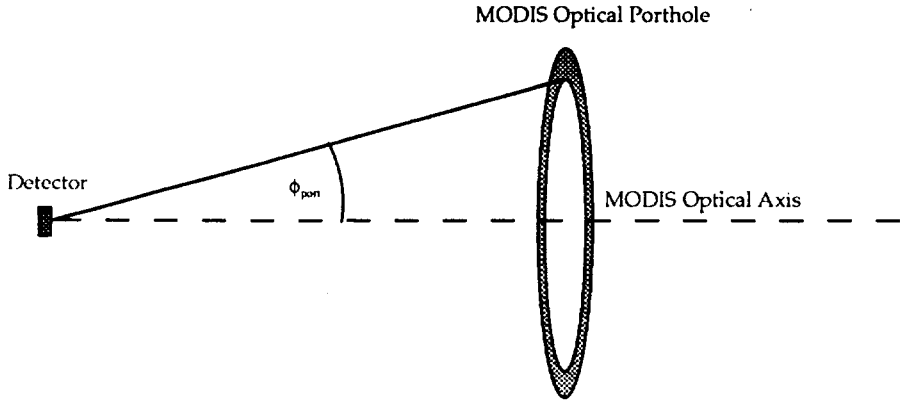

Figure 5. Effective Optical Acceptance Angle

4. Detector Flux Due To The Scan Mirror and Scene

Since MODIS has a revolving scan mirror in front of the optical system the effective transmission of the optical system will vary with scan angle. It is useful to consider two classes of optics: static and dynamic. Static optics are those lenses, mirrors, and filters from the first fold mirror to the detector which do not vary their tranmission properties between calibrators by changing their angular orientation. Dynamic optics refers to the scan mirror which views the blackbody, cold space, and the Earth at differing angles of incidence. This will result in significantly differing optical reflectance properties for each of the calibrators and the Earth scene.

Since it is not practical to express real transmission data in functional form, the detector flux equation is best expressed in summation form. Treating the radiance exiting the MODIS scan mirror (which has a reflectivity of $\rho_{\lambda,s}$) as a Lambertian source, Eq. 2 becomes

$$\Phi_s = \frac{\pi A_d}{4\left(f^{\#}_{eff}\right)^2_{port}} \sum_{\lambda=\lambda_1}^{\lambda_n} \left(\left(1-\rho^{on-orbit}_{\lambda,s}\right)B_{\lambda,mir} + \rho^{on-orbit}_{\lambda,s}L_{\lambda,s}\right)\tau^{on-orbit}_{\lambda,s}\Delta\lambda \tag{4}$$

where $B_{\lambda,mir}$ is the blackbody Planck function of the scan mirror and $L_{\lambda,s}$ is the spectral radiance incident upon the scan mirror of the image source (scene).

The superscript "on-orbit" will be used to denote the actual on-orbit value, whereas the same term without the superscript refers to the pre-launch measured value. Rearranging this equation to group the scan mirror reflectivity terms yields

$$\Phi_s = \frac{\pi A_d}{4\left(f^{\#}_{eff}\right)^2_{port}} \sum_{\lambda=\lambda_1}^{\lambda_n} \left(B_{\lambda,mir} + \rho^{on-orbit}_{\lambda,s}\left(L_{\lambda,s} - B_{\lambda,mir}\right)\right)\tau^{on-orbit}_{\lambda,s}\Delta\lambda \tag{5}$$

Since, the optical properties will change over time, it is necessary to account for these changes relative to the pre-launch measured values. These changes occur in the form of optical contamination and optical temperature variations. In order to correct for these changes on-orbit, it is necessary to consider them spectrally uniform across the bandwidth of each band. Furthermore, the ground values for optical tranmission will most likely contain a certain amount of error. This measurement error is analogous to on-orbit transmission changes and is treated as such. Since the accountability for these on-orbit changes and ground measurement errors must be treated as a spectrally uniform change across the entire bandwidth, it is adviseable to get a reasonable measurement of the optical tranmission properties pre-launch to be used in the algorithm.

For this paper, the word "contamination" will be used loosely to denote the on-orbit ratio of the optical transmission or scan mirror reflectivity to the pre-launch measured values. We define the on-orbit contamination of the static optics as

$$k_{\lambda,opt} = \frac{\tau_{\lambda,opt}^{on-orbit}}{\tau_{\lambda,opt}} \tag{6}$$

The pre-launch transmission of the static optics can be expressed in terms of a normalized measurement

$$\tau_{\lambda,opt}^{on-orbit} = T_{opt}^{on-orbit} R_{\lambda,opt}^{on-orbit} \tag{7}$$

where the total pre-launch integrated transmittance of the static optics is

$$T_{opt}^{on-orbit} = \sum_{\lambda=\lambda_1}^{\lambda_n} k_{\lambda,opt}\tau_{\lambda,opt}\Delta\lambda \tag{8}$$

and the pre-launch normalized spectral transmittance of the static optics is

$$R_{\lambda,opt}^{on-orbit} = \frac{k_{\lambda,opt}\tau_{\lambda,opt}}{\sum_{\lambda=\lambda_1}^{\lambda_n} k_{\lambda,opt}\tau_{\lambda,opt}\Delta\lambda} \tag{9}$$

Using Eq. 6, the on-orbit transmission of the static optics is

$$\tau_{\lambda,opt}^{on-orbit} = k_{\lambda,opt} T_{opt} R_{\lambda,opt} \tag{10}$$

Applying Eq. 10 to Eq. 5, the detector flux due to the scene and the scan mirror can be expressed as

$$\Phi_s = \frac{\pi A_d}{4\left(f_{eff}^{\#}\right)_{port}^2} \sum_{\lambda=\lambda_1}^{\lambda_n} \left(B_{\lambda,mir} + \rho_{\lambda,s}^{on-orbit}\left(L_{\lambda,s} - B_{\lambda,mir}\right)\right) k_{\lambda,opt} T_{opt} R_{\lambda,opt}\Delta\lambda \tag{11}$$

Again, assuming the contamination of the static optics to be spectrally uniform across the bandwidth, an average value of the contamination term may be factored out of the summation. We may also factor out the total integrated pre-launch optical transmission, since it is not wavelength dependent. Therefore,

$$\Phi_s = \frac{\pi A_d T_{opt} \bar{k}_{opt}}{4\left(f_{eff}^{\#}\right)_{port}^2} \sum_{\lambda=\lambda_1}^{\lambda_n} \left(B_{\lambda,mir} + \rho_{\lambda,s}^{on-orbit}\left(L_{\lambda,s} - B_{\lambda,mir}\right)\right) R_{\lambda,opt}\Delta\lambda \tag{12}$$

where $\bar{k}_{opt}$ is specifically

$$\bar{k}_{opt} = \frac{\sum_{\lambda=\lambda_1}^{\lambda_n}\left(B_{\lambda,mir} + \rho_{\lambda,s}^{on-orbit}\left(L_{\lambda,s} - B_{\lambda,mir}\right)\right)\tau_{\lambda,opt}^{on-orbit}\Delta\lambda}{\sum_{\lambda=\lambda_1}^{\lambda_n}\left(B_{\lambda,mir} + \rho_{\lambda,s}^{on-orbit}\left(L_{\lambda,s} - B_{\lambda,mir}\right)\right)\tau_{\lambda,opt}\Delta\lambda} \tag{13}$$

The on-orbit scan mirror contamination can be expressed as

$$\delta_{\lambda,s} = \frac{\rho_{\lambda,s}^{on-orbit}}{\rho_{\lambda,s}} \tag{14}$$

Applying this to Eq. 12 yields

$$\Phi_s = \frac{\pi A_d T_{opt}\bar{k}_{opt}}{4\left(f_{eff}^{\#}\right)_{port}^2}\sum_{\lambda=\lambda_1}^{\lambda_n} B_{\lambda,mir}R_{\lambda,opt}\Delta\lambda + \frac{\pi A_d T_{opt}\bar{k}_{opt}}{4\left(f_{eff}^{\#}\right)_{port}^2}\sum_{\lambda=\lambda_1}^{\lambda_n}\delta_{\lambda,s}\rho_{\lambda,s}\left(L_{\lambda,s} - B_{\lambda,mir}\right)R_{\lambda,opt}\Delta\lambda \tag{15}$$

Assuming the scan mirror contamination to be spectrally uniform across the bandwidth, an average value of this term can be factored out to yield

$$\Phi_s = \frac{\pi A_d T_{opt}\bar{k}_{opt}}{4\left(f_{eff}^{\#}\right)_{port}^2}\sum_{\lambda=\lambda_1}^{\lambda_n} B_{\lambda,mir}R_{\lambda,opt}\Delta\lambda + \frac{\pi A_d T_{opt}\bar{k}_{opt}\bar{\delta}_s}{4\left(f_{eff}^{\#}\right)_{port}^2}\sum_{\lambda=\lambda_1}^{\lambda_n}\rho_{\lambda,s}\left(L_{\lambda,s} - B_{\lambda,mir}\right)R_{\lambda,opt}\Delta\lambda \tag{16}$$

where $\bar{\delta}_s$ is specifically

$$\bar{\delta}_s = \frac{\sum_{\lambda=\lambda_1}^{\lambda_n}\rho_{\lambda,s}^{on-orbit}\left(L_{\lambda,s} - B_{\lambda,mir}\right)R_{\lambda,opt}\Delta\lambda}{\sum_{\lambda=\lambda_1}^{\lambda_n}\rho_{\lambda,s}\left(L_{\lambda,s} - B_{\lambda,mir}\right)R_{\lambda,opt}\Delta\lambda} \tag{17}$$

5. The Detector Voltage / Irradiance Equation

Applying Eq. 16 to the pre-amplified voltage relationship (Eq. 1) yields

$$V_s = a\left(P_{back} + \frac{\pi A_d T_{opt}\bar{k}_{opt}}{4\left(f_{eff}^{\#}\right)_{port}^2}\sum_{\lambda=\lambda_1}^{\lambda_n} B_{\lambda,mir}R_{\lambda,opt}\Delta\lambda + \frac{\pi A_d T_{opt}\bar{k}_{opt}\bar{\delta}_s}{4\left(f_{eff}^{\#}\right)_{port}^2}\sum_{\lambda=\lambda_1}^{\lambda_n}\rho_{\lambda,s}\left(L_{\lambda,s} - B_{\lambda,mir}\right)R_{\lambda,opt}\Delta\lambda\right)^2$$
$$+b\left(P_{back} + \frac{\pi A_d T_{opt}\bar{k}_{opt}}{4\left(f_{eff}^{\#}\right)_{port}^2}\sum_{\lambda=\lambda_1}^{\lambda_n} B_{\lambda,mir}R_{\lambda,opt}\Delta\lambda + \frac{\pi A_d T_{opt}\bar{k}_{opt}\bar{\delta}_s}{4\left(f_{eff}^{\#}\right)_{port}^2}\sum_{\lambda=\lambda_1}^{\lambda_n}\rho_{\lambda,s}\left(L_{\lambda,s} - B_{\lambda,mir}\right)R_{\lambda,opt}\Delta\lambda\right) \tag{18}$$

Selectively grouping terms which can be considered invariant across a single scan yields

$$V_s = a\left(\frac{\pi A_d T_{opt}\bar{k}_{opt}}{4\left(f^{\#}_{eff}\right)^2_{port}}\right)^2\left(\frac{4P_{back}\left(f^{\#}_{eff}\right)^2_{port}}{\pi A_d T_{opt}\bar{k}_{opt}} + \sum_{\lambda=\lambda_1}^{\lambda_n} B_{\lambda,mir}R_{\lambda,opt}\Delta\lambda + \bar{\delta}_s\sum_{\lambda=\lambda_1}^{\lambda_n}\rho_{\lambda,s}\left(L_{\lambda,s} - B_{\lambda,mir}\right)R_{\lambda,opt}\Delta\lambda\right)^2$$
$$+b\left(\frac{\pi A_d T_{opt}\bar{k}_{opt}}{4\left(f^{\#}_{eff}\right)^2_{port}}\right)\left(\frac{4P_{back}\left(f^{\#}_{eff}\right)^2_{port}}{\pi A_d T_{opt}\bar{k}_{opt}} + \sum_{\lambda=\lambda_1}^{\lambda_n} B_{\lambda,mir}R_{\lambda,opt}\Delta\lambda + \bar{\delta}_s\sum_{\lambda=\lambda_1}^{\lambda_n}\rho_{\lambda,s}\left(L_{\lambda,s} - B_{\lambda,mir}\right)R_{\lambda,opt}\Delta\lambda\right) \quad (19)$$

Introducing a blackbody relative scan mirror contamination term $\bar{\delta}_{bb}$, we get

$$V_s = a\left(\frac{\pi A_d T_{opt}\bar{k}_{opt}\bar{\delta}_{bb}}{4\left(f^{\#}_{eff}\right)^2_{port}}\right)^2\left(\frac{4P_{back}\left(f^{\#}_{eff}\right)^2_{port}}{\pi A_d T_{opt}\bar{k}_{opt}\bar{\delta}_{bb}} + \frac{1}{\bar{\delta}_{bb}}\sum_{\lambda=\lambda_1}^{\lambda_n} B_{\lambda,mir}R_{\lambda,opt}\Delta\lambda + \frac{\bar{\delta}_s}{\bar{\delta}_{bb}}\sum_{\lambda=\lambda_1}^{\lambda_n}\rho_{\lambda,s}\left(L_{\lambda,s} - B_{\lambda,mir}\right)R_{\lambda,opt}\Delta\lambda\right)^2$$
$$+b\left(\frac{\pi A_d T_{opt}\bar{k}_{opt}\bar{\delta}_{bb}}{4\left(f^{\#}_{eff}\right)^2_{port}}\right)\left(\frac{4P_{back}\left(f^{\#}_{eff}\right)^2_{port}}{\pi A_d T_{opt}\bar{k}_{opt}\bar{\delta}_{bb}} + \frac{1}{\bar{\delta}_{bb}}\sum_{\lambda=\lambda_1}^{\lambda_n} B_{\lambda,mir}R_{\lambda,opt}\Delta\lambda + \frac{\bar{\delta}_s}{\bar{\delta}_{bb}}\sum_{\lambda=\lambda_1}^{\lambda_n}\rho_{\lambda,s}\left(L_{\lambda,s} - B_{\lambda,mir}\right)R_{\lambda,opt}\Delta\lambda\right) \quad (20)$$

Equation 20 is now arranged such that it can be reduced to three variables (calibration coefficients) which can be determined with three calibration sources. The three calibration coefficients are

$$L_o = \frac{4P_{back}\left(f^{\#}_{eff}\right)^2_{port}}{\pi A_d T_{opt}\bar{k}_{opt}\bar{\delta}_{bb}} + \frac{1}{\bar{\delta}_{bb}}\sum_{\lambda=\lambda_1}^{\lambda_n} B_{\lambda,mir}R_{\lambda,opt}\Delta\lambda \quad (21)$$

$$m = \frac{b\pi A_d T_{opt}\bar{k}_{opt}\bar{\delta}_{bb}}{4\left(f^{\#}_{eff}\right)^2_{port}} \quad (22)$$

$$q = a\left(\frac{\pi A_d T_{opt}\bar{k}_{opt}\bar{\delta}_{bb}}{4\left(f^{\#}_{eff}\right)^2_{port}}\right)^2 \quad (23)$$

Expressed in terms of these three terms, Eq. 20 becomes

$$V_s = q\left(L_o + \bar{\delta}_{s/bb}\sum_{\lambda=\lambda_1}^{\lambda_n}\rho_{\lambda,s}\left(L_{\lambda,s} - B_{\lambda,mir}\right)R_{\lambda,opt}\Delta\lambda\right)^2 + m\left(L_o + \bar{\delta}_{s/bb}\sum_{\lambda=\lambda_1}^{\lambda_n}\rho_{\lambda,s}\left(L_{\lambda,s} - B_{\lambda,mir}\right)R_{\lambda,opt}\Delta\lambda\right) \quad (24)$$

where for notational purposes

$$\bar{\delta}_{s/bb} = \frac{\bar{\delta}_s}{\bar{\delta}_{bb}} \quad (24a)$$

From Eq. 22 and Eq. 23 it can be noted that the nonlinear term, q, is

$$q = \alpha m^2 \quad (25)$$

where

$$\alpha = \frac{a}{b^2} \quad (26)$$

6. The Top-Level Calibration Equation

Expressed in terms of the three calibration coefficients (m, L_o, and α), Eq. 24 becomes

$$V_s = \alpha m^2 \left(L_o + \overline{\delta}_{s/bb} \sum_{\lambda=\lambda_1}^{\lambda_n} \rho_{\lambda,s} \left(L_{\lambda,s} - B_{\lambda,mir} \right) R_{\lambda,opt} \Delta\lambda \right)^2 + m \left(L_o + \overline{\delta}_{s/bb} \sum_{\lambda=\lambda_1}^{\lambda_n} \rho_{\lambda,s} \left(L_{\lambda,s} - B_{\lambda,mir} \right) R_{\lambda,opt} \Delta\lambda \right) \tag{27}$$

7. Determination of the Earth Scene Spectral Radiance

Applying Eq. 27 to the Earth scene yields

$$V_{ev} = \alpha m^2 \left(L_o + \overline{\delta}_{ev/bb} \sum_{\lambda=\lambda_1}^{\lambda_n} \rho_{\lambda,s} \left(L_{\lambda,ev} - B_{\lambda,mir} \right) R_{\lambda,opt} \Delta\lambda \right)^2 + m \left(L_o + \overline{\delta}_{ev/bb} \sum_{\lambda=\lambda_1}^{\lambda_n} \rho_{\lambda,s} \left(L_{\lambda,ev} - B_{\lambda,mir} \right) R_{\lambda,opt} \Delta\lambda \right) \tag{28}$$

Since the spectal signature for the Earth scene is not known, an average value of the Earth scene radiance must be factored out of the summation. This term is commonly referred to as the spectral radiance of the Earth scene and is the final product of the calibration algorithm. Eq. 28 now becomes

$$\begin{aligned} V_{ev} = \alpha m^2 & \left(L_o + \overline{\delta}_{ev/bb} \overline{L}_{ev} \sum_{\lambda=\lambda_1}^{\lambda_n} \rho_{\lambda,s} R_{\lambda,opt} \Delta\lambda - \overline{\delta}_{ev/bb} \sum_{\lambda=\lambda_1}^{\lambda_n} \rho_{\lambda,s} B_{\lambda,mir} R_{\lambda,opt} \Delta\lambda \right)^2 \\ & + m \left(L_o + \overline{\delta}_{ev/bb} \overline{L}_{ev} \sum_{\lambda=\lambda_1}^{\lambda_n} \rho_{\lambda,s} R_{\lambda,opt} \Delta\lambda - \overline{\delta}_{ev/bb} \sum_{\lambda=\lambda_1}^{\lambda_n} \rho_{\lambda,s} B_{\lambda,mir} R_{\lambda,opt} \Delta\lambda \right) \end{aligned} \tag{29}$$

where $\overline{L}_{ev}$ is specifically

$$\overline{L}_{ev} = \frac{\sum_{\lambda=\lambda_1}^{\lambda_n} L_{\lambda,ev} \rho_{\lambda,s} R_{\lambda,opt} \Delta\lambda}{\sum_{\lambda=\lambda_1}^{\lambda_n} \rho_{\lambda,s} R_{\lambda,opt} \Delta\lambda} \tag{30}$$

Solving Eq. 29 for the Earth scene spectral radiance yields

$$\overline{L}_{ev} = \frac{-1 + \sqrt{1 + 4\alpha V_{ev}} + 2\alpha m \left(-L_o + \overline{\delta}_{ev/bb} \sum_{\lambda=\lambda_1}^{\lambda_n} \rho_{ev} B_{\lambda,mir} R_{\lambda,opt} \Delta\lambda \right)}{2\alpha m \overline{\delta}_{ev/bb} \sum_{\lambda=\lambda_1}^{\lambda_n} \rho_{ev} R_{\lambda,opt} \Delta\lambda} \tag{31}$$

With only two on-orbit calibrators to calibrate the MODIS infrared bands, it is only possible to have two calibration "coefficients" on-orbit. For the three calibrator pre-launch thermal vacuum tests, it will be possible to have three calibration coefficients. Therefore, the non-linear coefficient, α, will be determined from the thermal vacuum tests and assumed constant for the life of the mission (unless a means is developed for the on-orbit determination of this value).

To determine the two on-orbit calibration coefficients (m and L_O), apply Eq. 27 to the space view and blackbody. This yields two equations with two unknowns. Solving for these unknowns we get

$$L_o = \frac{-1+\sqrt{1+4\alpha V_{sv}}}{2\alpha m} + \bar{\delta}_{sv/bb}\sum_{\lambda=\lambda_1}^{\lambda_n}\rho_{sv}B_{\lambda,mir}R_{\lambda,opt}\Delta\lambda \tag{32}$$

$$m = \frac{\sqrt{1+4\alpha V_{bb}}-\sqrt{1+4\alpha V_{sv}}}{2\alpha\left(\sum_{\lambda=\lambda_1}^{\lambda_n}\rho_{bb}\left(L_{\lambda,bb}-B_{\lambda,mir}\right)R_{\lambda,opt}\Delta\lambda + \bar{\delta}_{sv/bb}\sum_{\lambda=\lambda_1}^{\lambda_n}\rho_{sv}B_{\lambda,mir}R_{\lambda,opt}\Delta\lambda\right)} \tag{33}$$

8. Determination of $\bar{\delta}_{ev/bb}$ and $\bar{\delta}_{sv/bb}$ During a Full Spacecraft Roll

On-orbit, it is possible to create a scenario where $\bar{\delta}_{ev/bb}$ may be determined for all Earth view scan angles. To do this MODIS must view space through the Earth view port at a scan angle of -23.4 degrees which corresponds to the same angle of incidence, ϕ_{bb}, with the scan mirror as the blackbody (see Fig. 6). Since the detector footprint for these two scan angles is effectively identical in size, shape, and location on the scan mirror, this creates a situation where m and L_o can be calibrated without scan mirror dependencies. Therefore

$$\phi_{ev@bb} = \phi_{bb} \tag{34}$$

Likewise,

$$\phi_{ev@sv} = \phi_{sv} \tag{35}$$

Applying Eq. 27 to the view of cold space through the Earth viewport at the scan mirror angle which is to be contamination corrected (ev), yields

$$V_{ev} = \alpha m^2\left(L_o + \bar{\delta}_{ev/bb}\sum_{\lambda=\lambda_1}^{\lambda_n}\rho_{\lambda,ev}\left(L_{\lambda,ev}-B_{\lambda,mir}\right)R_{\lambda,opt}\Delta\lambda\right)^2 + m\left(L_o + \bar{\delta}_{ev/bb}\sum_{\lambda=\lambda_1}^{\lambda_n}\rho_{\lambda,ev}\left(L_{\lambda,ev}-B_{\lambda,mir}\right)R_{\lambda,opt}\Delta\lambda\right) \tag{36}$$

Solving for $\bar{\delta}_{ev/bb}$, yields

$$\bar{\delta}_{ev/bb} = \frac{-1+\sqrt{1+4\alpha V_{ev}}-2\alpha m L_o}{2\alpha m\sum_{\lambda=\lambda_1}^{\lambda_n}\rho_{ev}\left(L_{\lambda,ev}-B_{\lambda,mir}\right)R_{\lambda,opt}\Delta\lambda} \tag{37}$$

To determine the calibration coefficients, apply Eq. 27 to the blackbody (bb) and to the view of cold space through the Earth viewport at the blackbody equivalent scan mirror angle of incidence (ev@bb). This yields two equations with two unknowns. Solving for these unknowns we get

$$L_o = \frac{-1+\sqrt{1+4\alpha V_{ev@bb}}}{2\alpha m} + \sum_{\lambda=\lambda_1}^{\lambda_n}\rho_{bb}B_{\lambda,mir}R_{\lambda,opt}\Delta\lambda \tag{38}$$

$$m = \frac{\sqrt{1+4\alpha V_{bb}}-\sqrt{1+4\alpha V_{ev@bb}}}{2\alpha\sum_{\lambda=\lambda_1}^{\lambda_n}\rho_{bb}L_{\lambda,bb}R_{\lambda,opt}\Delta\lambda} \tag{39}$$

Since the corresponding space view angle of incidence, ϕ_{sv}, occurs in the Earth view, $\bar{\delta}_{sv/bb}$ is equal to $\bar{\delta}_{ev/bb}$ at that angle. However, since the space view will also view cold space during the spacecraft roll, $\bar{\delta}_{sv/bb}$ can be calculated directly from Equations 37 - 39 (replace "ev" with "sv").

Since detector flux variations with respect to scan angle while viewing space will be small it will be neccesary to adjust the applied electronic gains to more adequately fill the A/D converter dynamic range and acheive better resolution. It is not in our plan to adjust these gains on-orbit (except for special events), however the capability for adjustment is there and should be recognized. The DC restore should be adjusted based on to the maximum expected value of the blackbody radiance as opposed to the normal adjustment which is based on expected Earth pixel radiance.

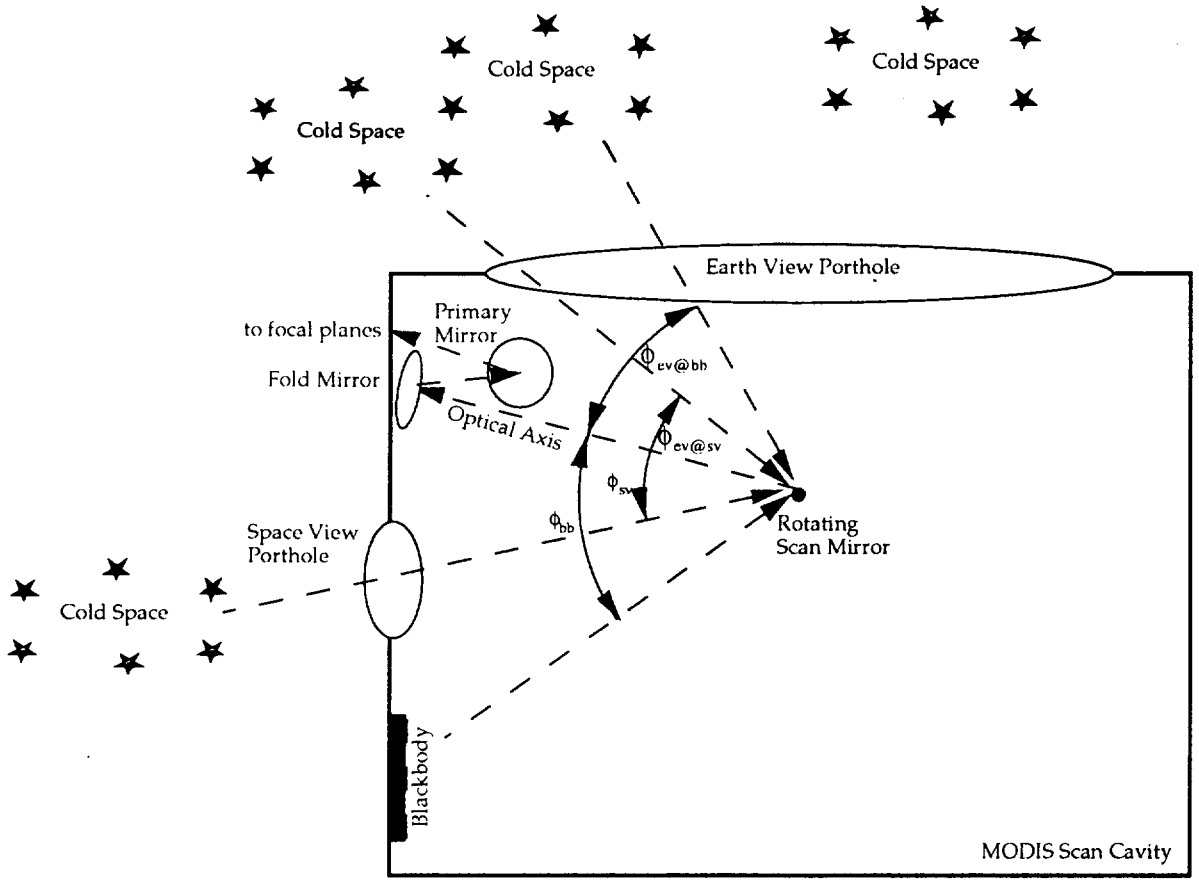

Figure 6. Scenario for deep space roll. Dashed line represents path of light ray to the detector. MODIS has an angle of incidence while viewing space through the Earth view porthole which is equivalent to the angle of incidence for each of the calibrators

9. Determination of the Pre-Launch Non-Linear Coefficient α

The thermal vacuum tests will use three calibration sources: the thermally isolated blackbody calibration source (bcs) at several temperatures and the space view source (svs). The nonlinear term can be determined for each pair of blackbody calibration source temperatures (bcs1 and bcs2). An average value for the nonlinear term can then be obtained. Applying the calibration equation (Eq. 27) to these three thermal vacuum calibrators results in three equations with three unknowns.

$$V_{bcs1} = q\left(L_{og} + \Delta L_{bcs1}\right)^2 + m\left(L_{og} + \Delta L_{bcs1}\right) \tag{40}$$

$$V_{bcs2} = q\left(L_{og} + \Delta L_{bcs2}\right)^2 + m\left(L_{og} + \Delta L_{bcs2}\right) \tag{41}$$

$$V_{svs} = q\left(L_{og} + \Delta L_{svs}\right)^2 + m\left(L_{og} + \Delta L_{svs}\right) \tag{42}$$

Where

$$\Delta L_{bcs1} = \sum_{\lambda=\lambda_1}^{\lambda_n} \rho_{\lambda,bcs1}\left(L_{\lambda,bcs1} - B_{\lambda,mir}\right)R_{\lambda,opt}\Delta\lambda \tag{43}$$

$$\Delta L_{bcs2} = \sum_{\lambda=\lambda_1}^{\lambda_n} \rho_{\lambda,bcs2}\left(L_{\lambda,bcs2} - B_{\lambda,mir}\right)R_{\lambda,opt}\Delta\lambda \tag{44}$$

$$\Delta L_{svs} = \sum_{\lambda=\lambda_1}^{\lambda_n} \rho_{\lambda,svs}\left(L_{\lambda,svs} - B_{\lambda,mir}\right)R_{\lambda,opt}\Delta\lambda \tag{45}$$

The variables m and q can then be obtained using determinants

$$m = \frac{A}{C} \tag{46}$$

$$q = \frac{B}{C} \tag{47}$$

Where

$$A = \begin{vmatrix} \left(\Delta L_{bcs1} + L_{og}\right)^2 & \left(V_{bcs1}\right) \\ \left(\Delta L_{bcs2} + L_{og}\right)^2 & \left(V_{bcs2}\right) \end{vmatrix} \tag{48}$$

$$B = \begin{vmatrix} \left(V_{bcs1}\right) & \left(\Delta L_{bcs1} + L_{og}\right) \\ \left(V_{bcs2}\right) & \left(\Delta L_{bcs2} + L_{og}\right) \end{vmatrix} \tag{49}$$

$$C = \begin{vmatrix} \left(L_{bcs1} + L_{og}\right)^2 & \left(L_{bcs1} + L_{og}\right) \\ \left(L_{bcs2} + L_{og}\right)^2 & \left(L_{bcs2} + L_{og}\right) \end{vmatrix} \tag{50}$$

Substitute Eq. 46 and Eq. 47 into Eq. 42

$$V_{svs} = \frac{B}{C}\left(\Delta L_{svs} + L_{og}\right)^2 + \frac{A}{C}\left(\Delta L_{svs} + L_{og}\right) \tag{51}$$

Eq. 51 can then be written as

$$B\left(\Delta L_{svs} + L_{og}\right)^2 + A\left(\Delta L_{svs} + L_{og}\right) - CV_{svs} = 0 \tag{52}$$

Solving for L_{og} yields

$$L_{og} = \frac{-y - \sqrt{y^2 - 4xz}}{2x} \tag{53}$$

Where

$$x = (\Delta L_{bcs2} - \Delta L_{bcs1})V_{svs} + (\Delta L_{bcs1} - \Delta L_{svs})V_{bcs2} + (\Delta L_{svs} - \Delta L_{bcs2})V_{bcs1} \quad (54)$$

$$y = (\Delta L^2_{bcs2} - \Delta L^2_{bcs1})V_{svs} + (\Delta L^2_{bcs1} - \Delta L^2_{svs})V_{bcs2} + (\Delta L^2_{svs} - \Delta L^2_{bcs2})V_{bcs1} \quad (55)$$

$$z = (\Delta L^2_{bcs2}\Delta L_{bcs1} - \Delta L^2_{bcs1}\Delta L_{bcs2})V_{svs} + (\Delta L^2_{bcs1}\Delta L_{svs} - \Delta L^2_{svs}\Delta L_{bcs1})V_{bcs2} + (\Delta L^2_{svs}\Delta L_{bcs2} - \Delta L^2_{bcs2}\Delta L_{svs})V_{bcs1} \quad (56)$$

I feel that the negative root of the quadratic may be the appropriate root to use in Eq. 53. This is determined based on a consideration of what happens when the flux due to the optical background increases while the flux due to the scan mirror and image sources remain constant. For this scenario the pre-amplified voltages will increase for all three calibrators. Due to this, c may change more so than a and b. For this case, L_{og} must increase as z increases and the negative root must be used, except when x<0, y>0 and z<0.

However, since L_{og} is only determined pre-launch, it would be better and safer to determine the sign of the root by applying the thermal vacuum data to Eq. 53 for both signs of the root and using the root resulting in the greater value of L_{og}. Since L_{og} is defined as positive in the on-orbit algorithm this would insure the use of the correct root of Eq. 53.

From Equation 26 we see that

$$\alpha = \frac{q}{m^2} \quad (57)$$

Plugging Eq. 46 and Eq. 47 into Eq. 57 gives

$$\alpha = \frac{BC}{A^2} \quad (58)$$

Therefore the pre-launch calibration coefficient α is

$$\alpha = \frac{\left(V_{bcs1}(\Delta L_{bcs2} + L_{og}) - V_{bcs2}(\Delta L_{bcs1} + L_{og})\right)\left((L_{bcs2} + L_{og})(L_{bcs1} + L_{og})^2 - (L_{bcs1} + L_{og})(L_{bcs2} + L_{og})^2\right)}{\left(V_{bcs2}(\Delta L_{bbs1} + L_{og})^2 - V_{bcs1}(\Delta L_{bcs2} + L_{og})^2\right)^2} \quad (59)$$

The blackbody calibration source will be adjusted to several temperatures. Since it is thermally isolated from MODIS, these reference values may be used in addition to the space view source to determine α. In this case, Eq. 59 might be rewritten replacing bcs with bcs1 and bbs with bcs2. Eq. 59 could then be applied to each pair of blackbody calibration source temperature levels to determine an average value of α to be used on-orbit.

It is planned to measure α at several patch and optics temperatures. This will enable us to apply the appropriate value by measuring the patch and optics temperatures on-orbit. Theoretically α should vary little with optics temperature. This will determined from the protoflight data. If trending of α occurs in the protoflight tests, attempts will be made to trace this back to individual data parameters in an effort to correct for changes in α on-orbit

10. Determination of the On-Board Blackbody Spectral Radiance

The 12 thermistor readings will be averaged to obtain one temperature for the blackbody, T_{bb}. With a knowledge of the expected temperature gradients of the blackbody, an algorithm will be developed to identify faulty thermistors. Any thermistors which sufficiently deviate from the mean will not be used in the determination of the average blackbody temperature.

The spectral radiance of the blackbody incident on the scan mirror can be determined every scan as

$$L_{\lambda,bb} = \varepsilon_{bb} B_{\lambda,bb} + \frac{1-\varepsilon_{bb}}{\pi}\left(\Omega_{cav} B_{\lambda,cav} + \Omega_{ev} B_{\lambda,Earth}\right) \quad (60)$$

where:

$$\Omega_{cav} + \Omega_{ev} = \pi \tag{61}$$

ε_{bb} = blackbody emissivity (measured pre-launch)
Ω_{cav} = effective solid angle of the scan cavity subtended at the blackbody
Ω_{ev} = effective solid angle of the Earth view porthole visible to the blackbody

Note the use of the notation ε_{bb} to denote the emissivity of the blackbody itself, and ρ_{bb} to denote the reflectivity of the scan mirror at the blackbody view angle. For the purposes of simple (but specific) notation in this document, refectivity ρ will be tied to the mirror and emissivity ε will be tied to the Planck source viewed by the scan mirror at a particular angle. Thermal vacuum data will use the blackbody calibration source to calibrate the on-board blackbody. This algorithm is TBD and will determine how the scan cavity temperature is calculated.

The effective temperature of the scan cavity must be determined from appropriate thermistors within the scan cavity. This algorithm is currently TBD.

The effective temperature of the Earth is a fairly minor term in Eq. 60. This temperature refers to an average temperature of the entire Earth scene which illuminates the surface of the on-board blackbody. This algorithm is currently TBD.

11. Determination of the Planck Function Spectral Radiance $B_{\lambda,s}$

Since the desired units of spectral radiance is Watts per meter squared per micron per steradian, the Planck function is:

$$B_{\lambda,s} = \frac{2hc^2}{\pi\lambda^5\left(e^{(ch/\lambda kT_s)} - 1\right)} \tag{62}$$

where:

h = Planck's constant $6.6256 \pm 0.0005 \times 10^{-34}$ W sec^2
c = Speed of light $2.997925 \pm .000003 \times 10^{8}$ m / sec
k = Boltzmann's constant $1.38054 \pm 0.00018 \times 10^{-23}$ W sec / K
Ts = temperature of the Planck source (i.e. scan mirror, blackbody, scan cavity, blackbody calibration source, etc.)

12. Determination of the Pre-Amplified Detector Voltages

The following are the current MCST algorithms for converting the MODIS digital number output of the analog to digital (A/D) converter into the pre-amplified voltages. These algorithms are essential to the master curve approach since a digital number by itself has no meaning without its respective applied gains and offsets.

The pre-amplified voltages will be determined in three modular steps. The first module determines the A/D converter coefficients based on on-orbit and/or pre-launch measurements. The second module converts the MODIS digital number output of the A/D converter into the voltage input of the A/D converter. The third module converts the voltage input of the A/D converter into the pre-amplified voltages. There is a distinct third modular stage for both the photovoltaic and the photoconductive bands due to their differing electronic configuration. Figure 7 outlines these modules with their respective input and output parameters.

12-1. Electronic Calibration

The on-orbit and pre-launch approaches to determining the coeffiecents of A/D responsivity are TBD for this memorandum.

12-2. Determination of the Amplified Voltage Input to A/D Converter

The functionality of the A/D output (DN) with respect to the input voltage ($V_{A/D}$) will be analyzed to determine the best fit to use. This fit will currently be represented as an Nth order polynomial.

$$V_{A/D} = \sum_{n=1}^{N} a_n (DN - DN_o)^n \tag{63}$$

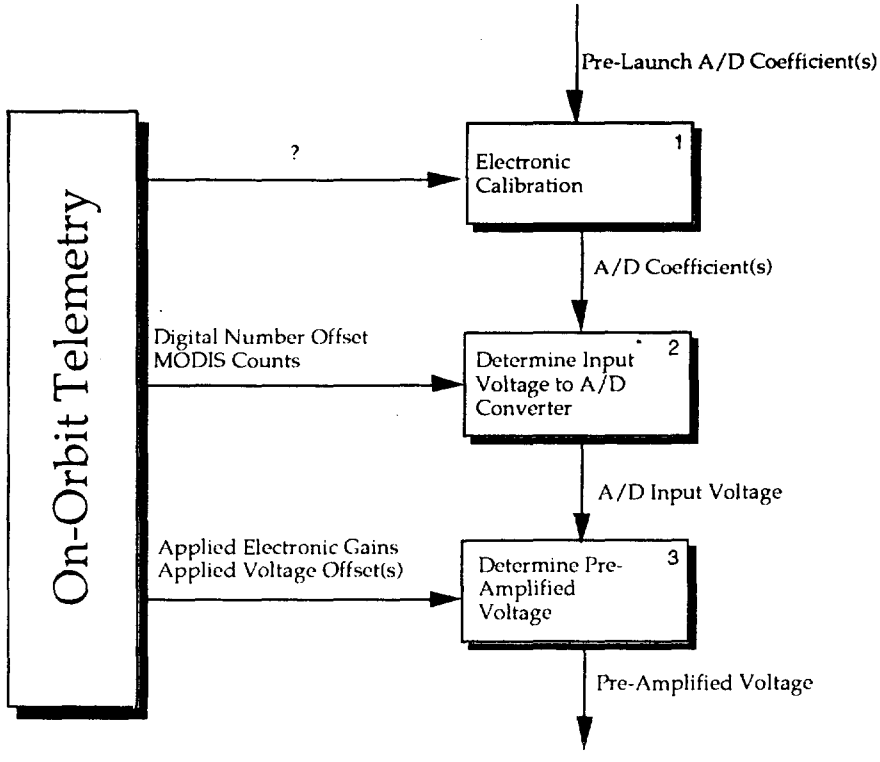

Figure 7. Outline of Pre-Amplified Voltage Determination Algorithm

12-3. Determination of the Pre-Amplified Voltage

To remove the applied electronic gains and offsets from the MODIS signal, it is neccesary develop two algorithms: one for the photoconductive bands and one for the photovoltaic bands. The PV bands have four applied gain and one applied offset (see Fig. 8). The PC bands have two applied gains and two applied offsets (see Fig. 9). The offset for the PC bands is higher than for the PV bands since the detector flux due to the optical system is greater for higher wavelengths. Therefore, the PC circuit configuration must have two offsets to acheive an offset resolution comparable to that of the PV bands. The first PC offset is the course adjustment and the second PC offset is the fine adjustment.

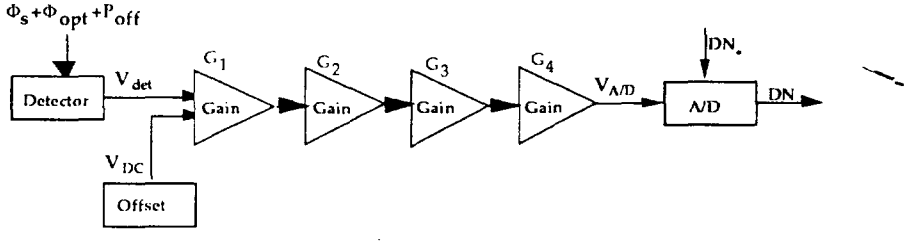

Figure 8. Electronics circuit design for the photovoltaic bands

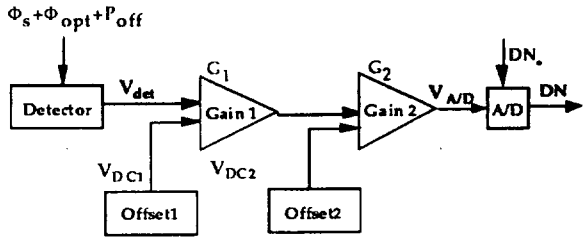

Figure 9. Electronics circuit design for the photoconductive bands

To calibrate the photovoltaic bands, the pre-amplified voltage across the detector will be used, since it increases with detector flux. From the electronics circuit of Figure 8, we can see that

$$V_s^{PV} = \frac{V_{A/D}}{G_1 G_2 G_3 G_4} - V_{DC1} \tag{64}$$

To calibrate the photoconductive bands, the pre-amplified voltage across the load resistor will be used, since it increases with detector flux. From the electronics circuit of Figure 9, we can see that

$$V_s^{PC} = \frac{V_{A/D}}{G_1 G_2} - \frac{V_{DC2}}{G_1} - V_{DC1} \tag{65}$$

The superscript notation "PV" and "PC" is used here to more readily distinguish the appropriate equation for each detector circuit. It is important to note that the actual value for V_{DC1} and V_{DC2} will be negative.